Nonlinear Analysis: Modelling and Control, Vol. 30, No. 5, 874–891
https://doi.org/10.15388/namc.2025.30.42247

# A mathematical model for degradation of forest area by industrialization causing migration of wildlife species

**Shikha Jatav**[a, 1], **Shyam Sundar**[b], **Alok Malviya**[c]

[a] Department of Mathematics, Lajpat Rai College,
Sahibabad, Ghaziabad, UP 201005, India
shikhajatav0512@gmail.com

[b] Department of Mathematics,
Pranveer Singh Institute of Technology,
Kanpur, UP 209305, India
ssmishra15@gmail.com

[c] Department of Mathematics, VSSD (PG) College,
Kanpur, UP 208002, India
alok92nov@gmail.com

**Received:** January 2, 2025 / **Revised:** April 28, 2025 / **Published online:** June 5, 2025

**Abstract.** This study presents a nonlinear mathematical model incorporating four key variables: forest area, biomass density, industrialization level, and wildlife population. The model assumes that biomass is proportional to forest area and that wildlife density depends on biomass availability. Our analysis demonstrates that increasing industrialization leads to significant forest depletion, which in turn accelerates wildlife migration. The results highlight critical thresholds beyond which forest degradation becomes irreversible, emphasizing the urgent need for sustainable industrial policies and conservation strategies. Numerical simulations and sensitivity analysis validate the model outcomes and provide insights for ecological preservation.

**Keywords:** forest area, industrialization, migration, wildlife species, stability analysis.

## 1 Introduction

Approximately 31% of the Earth's land area is covered by forests, playing a vital role in sustaining human life through their contributions to water and air purification, as well as the provision of essential food and medicinal resources [27]. Forests play a crucial role in supporting diverse ecosystems, as evidenced by the fact that approximately 80% of the world's land-based species, including iconic animals, like elephants and rhinos, rely on these habitats. Deforestation, primarily driven by factors, such as poorly planned infrastructure for agriculture, illegal logging, and industrialization, poses a significant threat

[1] Corresponding author.

to these ecosystems [23, 24]. In today's context, the increasing pace of industrialization and the associated pollution pose a significant challenge. Although the industrial revolution has unquestionably improved our lives and streamlined various processes, it has simultaneously led to a host of problems. These issues encompass a rise in harmful gases and particles, the presence of toxic substances, the reduction of forestry resources, and the displacement of wildlife species [21, 26].

Wood is a key raw material for industries producing plywood, paper, furniture, packaging, and more. This high demand puts immense pressure on forests, making overexploitation a major cause of forest degradation [28]. As forests shrink, wildlife habitats are destroyed, prompting continuous species migration [25]. Over the past decades, many plants and animals have been lost due to this trend. Industrial deforestation, driven by logging, mining, agriculture, and infrastructure, is rapidly expanding due to global industrial growth. The rising demand for timber, paper, palm oil, soy, and minerals leads to massive forest clearing. Farmers are also pushed to increase output for raw materials needed by industries. According to FAO, 7.3 million hectares of forest are lost annually to industrial deforestation. At the current rate, global rainforests may face complete destruction, with forests vanishing at the rate of a football field every two seconds [22].

In recent decades, rising industrialization has intensified stress on forest resources and wildlife. Several researchers have examined this degradation and proposed conservation strategies [6, 10–12, 16, 20]. Lata et al. [10] modeled forest pollution from wood and nonwood industries, showing that increased activity threatens sustainability. Jyotsna and Tandon [9] highlighted the impact of human actions on biomass loss and wildlife, urging sustainable mining. Shukla et al. [18] developed a nonlinear model linking resource depletion to population and industrial growth, warning of extinction risks without technological conservation. Misra and Jha [14] showed that population pressure severely affects forest biomass.

Agrawal et al. [1] proposed a model analyzing interactions among forestry biomass, industrialization, and wildlife, recommending green cover preservation and regulated industrial growth for wildlife sustainability. Studies [4, 13, 17] identify population pressure as a key driver of industrialization. Dubey et al. [4] used a nonlinear model to show that combined population and industrial growth significantly degrades forests, calling for balanced development. Misra et al. [13] showed that rising industrialization, even with partial population dependence on resources, can lead to resource extinction. Economic strategies to reduce population pressure help conserve forests. Research links resource-based industries to declining forest cover [10]. Shukla et al. [19] highlighted that intensified industrialization lowers forest density, threatening wildlife, and stressed conserving biomass. Upadhyay et al. [5] examined how population growth, pollution, and industry harm forest sustainability. Jha and Misra [8] found environmental taxes effective in curbing environmental degradation.

It is important to note from the previous discussion that increasing population growth and industrialization are major factors in the depletion of forestry resources, which puts wildlife species survival at risk. Given this, the current study considers how industrialization damages forest areas and drives wildlife migration, which is totally reliant on the biomass density of forestry resources. To investigate this, in the present research work, a nonlinear mathematical model is introduced and analyzed. The model uniquely captures the dynamic between industrialization and forest degradation, incorporating cumulative biomass density as a key factor. It highlights a nonlinear relationship where species displacement is driven by both habitat loss and biomass decline, offering a more integrated view than previous studies. The literature on industrialization-induced deforestation and wildlife migration has evolved from focusing on direct biodiversity loss to using dynamic, system-based models that integrate ecological, economic, and policy factors. Current research emphasizes holistic approaches, though challenges remain in capturing complex interactions and translating findings into effective, actionable conservation strategies.

This work introduces a dynamic ecological-industrial framework, integrating industrial growth, forest degradation, and wildlife migration. It uniquely incorporates cumulative biomass density as a key factor influencing species displacement and establishes a nonlinear relationship between industrialization and wildlife migration. The model also identifies critical thresholds for irreversible forest loss, offering insights into sustainable industrial policies.

## 2 Mathematical model

The model addresses wildlife migration caused by forest degradation, assuming forest biomass density depends on forest size and solely determines animal populations, both threatened by rising industrialization.

Let $F(t)$ represent the forest area at any time $t$. $B(t)$ denotes the cumulative biomass density of forest resources in the region under consideration at any time $t$. $I(t)$ represents the level of industrialization at any time $t$ in the same region. $W(t)$ signifies the wildlife species density at any time $t$ in the same area. Based on the assumptions outlined above, a schematic diagram illustrating the problem is presented in Fig. 1, and the corresponding model equations are derived as follows:

$$\begin{aligned}
\frac{\mathrm{d}F}{\mathrm{d}t} &= q - \alpha_0(F - F_0) - \alpha_1 IF,\\
\frac{\mathrm{d}B}{\mathrm{d}t} &= sF - s_0B - kBW,\\
\frac{\mathrm{d}I}{\mathrm{d}t} &= \mu\alpha_1 IF - \mu_0 I^2,\\
\frac{\mathrm{d}W}{\mathrm{d}t} &= \pi kBW - \pi_0 W - \pi_1 W^2 - \pi_2 WI,
\end{aligned} \tag{1}$$

here $F(0) \geqslant 0$, $B(0) \geqslant 0$, $I(0) \geqslant 0$, and $W(0) \geqslant 0$. All parameters in this context are considered to be positive.

In the first equation, $q$ represents the rate of increase of forest area due to reforestation, and $\alpha_0$ denotes the rate of forest depletion by natural factors. $F_0$ is the reserved forest area. As discussed above, industrialization contributes to forest area depletion through activities like logging, agriculture expansion, mining, infrastructure development, urbanization, and energy production. Therefore, it is reasonable to assume $\alpha_1$ as the rate of forest

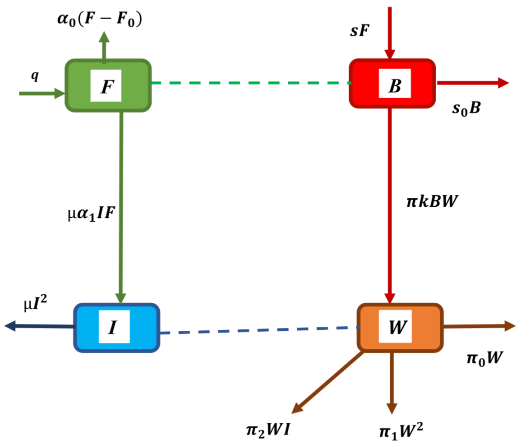


**Figure 1.** Schematic diagram for the model system (1).

depletion by industrialization. With the assumption that the growth of biomass density is proportionate to the forest area, $s$ denotes the growth rate of biomass density in the second equation. The consumption rate of forest resources by wildlife species is represented by $k$, while the natural depletion rate of forest resources is indicated by the constant $s_0$. In the third equation, the term $\mu\alpha_1 IF$ shows the growth of industrialization with proportionality constant $\mu$ due to the effect of forest area. The constant $\mu_0$ corresponds to the intraspecific coefficient among industries. We assume that wildlife species in the fourth equation are totally reliant on forest resources. With a proportionality constant of $\pi$, the expansion of wildlife species as a result of forest resources is represented by the term $\pi kBW$. The quantity $\pi_1 W^2$ indicates a decline in the density of wildlife species as a result of death brought on by crowding at a rate of $\pi_1$. The constant $\pi_0$ represents the natural depletion rate. The rate coefficient at which animal species migrate as a result of rising civilization is $\pi_2$. This model extends previous works by explicitly linking industrial growth, forest degradation, and wildlife migration within a unified mathematical framework. Unlike previous studies, this approach integrates industrial growth with ecological dynamics, using biomass as a central variable to demonstrate how industrialization nonlinearly reduces forest cover and accelerates wildlife migration.

**Remark 1.** From last equation of the model system (1) it is evident that, in the presence of industrialization, the intrinsic growth rate of wildlife species for any time $t > 0$ is $\pi kB - \pi_0 - \pi_2 I$. For the model system to be feasible, $\pi kB - \pi_0 - \pi_2 I$ must remain positive for all times $t > 0$. The condition $\pi kB - \pi_0 - \pi_2 I > 0$ ensures that the wildlife population can grow and remain viable. It means that the biomass density ($B$) must be sufficient to support the species, as it provides food and habitat. However, growth is limited by natural mortality ($\pi_0$) and the negative impacts of industrialization ($\pi_2 I$), which disrupt ecosystems and reduce habitat quality. For the wildlife to thrive, the available biomass must outweigh these negative factors, ensuring a positive growth rate and long-term sustainability.

# 3 Model analysis

## 3.1 Boundedness of the system

Ensuring the boundedness of the model system is crucial for its analysis. To achieve this, we rely on the following lemma, which assures the boundedness of the model system, thus enabling us to proceed with our investigation.

**Lemma 1.** *The set*

$$\Omega = \{(F, B, I, W)\colon\ 0 \leqslant F \leqslant F_m,\ 0 \leqslant B \leqslant B_m,\ 0 \leqslant I \leqslant I_m,\ 0 \leqslant W \leqslant W_m\}, \quad (2)$$

*where* $F_m = (q + \alpha_0 F_0)/\alpha_0$, $B_m = sF_m/s_0$, $I_m = \mu\alpha_1 F_m/\mu_0$, $W_m = (\pi k B_m - \pi_0)/\pi_1 > 0$, *forms the domain of attraction for the model system, drawing all solutions originating within the interior of the positive orthant toward it* [7, 15].

## 3.2 Equilibrium analysis

The aforementioned model system possesses four equilibria, all of which are nonnegative:

$$E_1\left(\frac{q+\alpha_0F_0}{\alpha_0}, \frac{s(q+\alpha_0F_0)}{\alpha_0 s_0}, 0, 0\right), \quad E_2\left(\frac{q+\alpha_0F_0}{\alpha_0}, B_2, 0, W_2\right),$$
$$E_3(F_3, B_3, I_3, 0), \quad \text{and} \quad E^*(F^*, B^*, I^*, W^*),$$

where

$$B_2 = \frac{-(s_0 - \frac{k\pi_0}{\pi_1}) + \sqrt{(s_0 - \frac{k\pi_0}{\pi_1})^2 + 4\frac{\pi k^2}{\pi_1} s(\frac{q+\alpha_0F_0}{\alpha_0})}}{\frac{2\pi k^2}{\pi_1}}, \quad W_2 = \frac{\pi k B_2 - \pi_0}{\pi_1},$$

$$F_3 = \frac{-\alpha_0 + \sqrt{\alpha_0^2 + 4\frac{\mu\alpha_1^2}{\mu_0}(q+\alpha_0F_0)}}{\frac{2\mu\alpha_1^2}{\mu_0}}, \quad B_3 = \frac{sF_3}{s_0}, \quad \text{and} \quad I_3 = \frac{\mu\alpha_1F_3}{\mu_0}.$$

In the following, we illustrate the existence of the equilibrium $E^*$.

*Existence of $E^*$.* The equilibrium $E^*$ is obtained by solving these equations:

$$q - \alpha_0(F - F_0) - \alpha_1 F I = 0, \quad (3)$$
$$sF - s_0B - kBW = 0, \quad (4)$$
$$\mu\alpha_1 F - \mu_0 I = 0, \quad (5)$$
$$\pi k B - \pi_0 - \pi_1 W - \pi_2 I = 0. \quad (6)$$

Solving Eqs. (3) and (5), we get

$$F = \frac{-\alpha_0 + \sqrt{\alpha_0^2 + 4\frac{\mu\alpha_1^2}{\mu_0}(q+\alpha_0F_0)}}{\frac{2\mu\alpha_1^2}{\mu_0}} = F^* \ \text{(say)}$$

and

$$I = \frac{\mu\alpha_1 F^*}{\mu_0} = I^* \text{ (say)}.$$

From Eq. (6) we get

$$W = \frac{(\pi k B - \pi_0 - \pi_2 I^*)}{\pi_1}. \tag{7}$$

Substituting the values of $W$ and $F$ into Eq. (4), we obtain

$$\frac{\pi k^2}{\pi_1} B^2 + \left[s_0 - k\left(\frac{\pi_0 + \pi_2 I^*}{\pi_1}\right)\right] B - sF^* = 0.$$

This equation has unique positive root, $B = B^*$. From Eq. (6) we get

$$W = \frac{(\pi k B^* - \pi_0 - \pi_2 I^*)}{\pi_1} = W^* \text{ (say)}.$$

This indicates that the equilibrium $E^*$ exists uniquely.

# 4 Stability analysis

## 4.1 Local stability analysis

Local stability studies how a system behaves close to an equilibrium point, focusing on how slight deviations from the equilibrium affect the dynamics of the system. To analyze the dynamics of the system and predict its behavior in the immediate region of an equilibrium point, it is imperative to evaluate the local stability near an equilibria. We construct a Jacobian matrix for the provided model system to discern the characteristics of local stability at an equilibrium point.

Below is the Jacobian matrix associated with the model system (1):

$$J = \begin{bmatrix} -\alpha_0 - \alpha_1 I & 0 & -\alpha_1 F & 0 \\ s & -s_0 - kW & 0 & -kB \\ \mu\alpha_1 I & 0 & \mu\alpha_1 F - 2\mu_0 I & 0 \\ 0 & \pi k W & -\pi_2 W & \pi k B - \pi_0 - 2\pi_1 W - \pi_2 I \end{bmatrix}.$$

In the case of equilibrium $E_1$, the eigenvalues of $J$ are $-\alpha_0$, $-s_0$, $\mu\alpha_1((q + \alpha_0 F_0)/\alpha_0)$, $\pi ks((q+\alpha_0 F_0)/(s_0\alpha_0))-\pi_0$. In this context, it is observed that two eigenvalues, denoted as $\mu\alpha_1((q + \alpha_0 F_0)/\alpha_0)$ and $\pi ks((q + \alpha_0 F_0)/(s_0\alpha_0)) - \pi_0$, are positive. Consequently, the equilibrium point $E_1$ is consistently unstable in $IW$-plane.

(i) *Unstable equilibrium* $E_1$. This suggests that without industrialization or wildlife species, even minimal industrial activity or wildlife introduction will push the system away from this equilibrium. Conservation policies should focus on preventing total deforestation to avoid a situation where forests and biomass are present, but unable to support either biodiversity or industrial activity.

(ii) *Unstable equilibrium* $E_2$. For the Jacobian matrix $J$ associated with $E_2$, it is observed that one eigenvalue $\mu\alpha_1((q + \alpha_0 F_0)/\alpha_0)$ is positive. Consequently, equilibrium $E_2$ is consistently unstable in $I$-direction. This suggests that a system with forest, biomass, and wildlife but no industrialization is not sustainable, as industrialization naturally emerges over time. Conservation efforts should focus on regulating industrial expansion rather than assuming a purely natural state can persist indefinitely.

Of the Jacobian matrix $J$ pertaining to $E_3$, it is observed that one eigenvalue $\pi k B_3 - \pi_0 - \pi_2 I_3$ must be positive for the feasible of $E^*$. Thus, there exists a positive eigenvalue and equilibrium $E_3$ is unstable whenever $E^*$ is feasible. As a result, equilibrium $E_3$ remains inconsistently unstable and stable in $W$-direction.

In the following, to stabilize local stability condition, we consider the positive definite function, where $x_1$, $x_2$, $x_3$, and $x_4$ are minor perturbations around the equilibrium $E^*$. Now, contemplate a the positive definite function expressed as

$$U = \frac{1}{2}\left(x_1^2 + k_1 x_2^2 + \frac{k_2 x_3^2}{I^*} + \frac{k_3 x_4^2}{W^*}\right), \tag{8}$$

here $k_1$, $k_2$, and $k_3$ denote positive constants that must be selected suitably. We use linearized system of the model about the equilibrium $E^*$ and choose

$$k_1 < \frac{(\alpha_0 + \alpha_1 I^*)(s_0 + kW^*)}{s^2}, \qquad k_2 = \frac{F^*}{\mu},$$

and

$$k_3 < \min\left[\frac{B^*(\alpha_0 + \alpha_1 I^*)(s_0 + kW^*)}{\pi s^2}, \frac{F^* \pi_1 \mu_0}{\mu \pi_2^2}\right].$$

The fact that $\mathrm{d}U/\mathrm{d}t$ is negative definite without any condition demonstrates that $U$ acts as a Lyapunov function, thereby confirming Theorem 1.

**Theorem 1.**

(i) *Equilibria $E_1$ and $E_2$ are always unstable.*

(ii) *Equilibrium $E_3$ is stable when $\pi_2 > (\pi_1 k B_3 - \pi_0)/I_3$ and become unstable whenever $E^*$ exists.*

(iii) *Equilibrium $E^*$ exhibits local asymptotic stability unconditionally.*

**Remark 2.** Theorem 1 suggests that the system will converge to the equilibrium point $E^*$ within a specific region of initial conditions surrounding the equilibrium point $E^*$.

(iii) *Stability of the equilibrium* $E_3$. The equilibrium, which is stable when $\pi_2 < (\pi_1 k B_3 - \pi_0)/I_3$, implies that conservation policies must ensure that industrial activities do not exceed certain value. If industrialization increases beyond these limits, it can destabilize the system, leading to forest depletion and loss of biodiversity. Therefore, regulation of industrial growth and promoting sustainable practices are crucial to maintaining forest and biomass stability.

On the other hand, the equilibrium $E^*$, which is locally asymptotically stable without any condition, implies that this equilibrium can be naturally achieved and maintained by the system. For conservation policies, this suggests that efforts should focus on promoting balanced interactions between industrialization, forest conservation, and wildlife preservation. Sustainable land-use planning, wildlife corridors, and eco-friendly industrial practices would help ensure that the system remains in this stable state, fostering long-term ecological and industrial sustainability.

Overall, the findings emphasize the need for balanced industrial policies, habitat protection, and sustainable land-use strategies to maintain both economic development and ecological stability.

### 4.2 Global stability analysis

When an equilibrium point in a dynamic system is globally stable, it means that, under any beginning conditions, the system's trajectory will ultimately converge to the equilibrium point and stay within a stable region of attraction over time. To establish the equilibrium $E^*$, we introduce the following positive definite function centered around $E^*$:

$$V(F,B,I,W) = \frac{1}{2}(F-F^*)^2 + \frac{m_1}{2}(B-B^*)^2 + m_2\left(I - I^* - I^*\log\frac{I}{I^*}\right) + m_3\left(W - W^* - W^*\log\frac{W}{W^*}\right), \tag{9}$$

where $m_1, m_2, m_3 > 0$ and can be chosen appropriately. It is evident that the function $V$ vanishes at the equilibrium $E^*$ and is positive for any other positive values of $F$, $B$, $I$, and $W$.

The differentiation of equation (9) is given as

$$\frac{\mathrm{d}V}{\mathrm{d}t} = (F-F^*)\frac{\mathrm{d}F}{\mathrm{d}t} + m_1(B-B^*)\frac{\mathrm{d}B}{\mathrm{d}t} + m_2\left(1-\frac{I^*}{I}\right)\frac{\mathrm{d}I}{\mathrm{d}t} + m_3\left(1-\frac{W^*}{W}\right)\frac{\mathrm{d}W}{\mathrm{d}t}.$$

By substituting the derivatives obtained from Eqs. (1) and simplifying, we arrive at

$$\begin{aligned}\frac{\mathrm{d}V}{\mathrm{d}t} &= -(\alpha_0+\alpha_1 I)(F-F^*)^2 - m_1(s_0+kW)(B-B^*)^2 \\ &\quad - m_2\mu_0(I-I^*)^2 - m_3\pi_1(W-W^*)^2 - (F^*-\mu m_2)\alpha_1(F-F^*)(I-I^*) \\ &\quad + sm_1(B-B^*)(F-F^*) - (m_1B^* - m_3\pi)k(B-B^*)(W-W^*) \\ &\quad - \pi_2 m_3(I-I^*)(W-W^*).\end{aligned}$$

Now choose

$$m_1 < \frac{\alpha_0 s_0}{s^2}, \quad m_2 = \frac{F^*}{\mu}, \quad \text{and} \quad m_3 < \min\left[\frac{B^*\alpha_0 s_0}{\pi s^2}, \frac{F^*\pi_1\mu_0}{\mu\pi_2^2}\right].$$

The fact that $\mathrm{d}V/\mathrm{d}t$ is negative definite within the region of attraction $\Omega$ demonstrates that $V$ serves as a Lyapunov function, thereby substantiating Theorem 2 without the need for any additional conditions.

**Theorem 2.** *The equilibrium $E^*$ exhibits global asymptotic stability without any additional conditions.*

**Remark 3.** Theorem 2 suggests that the equilibrium $E^*$ exerts a universal attraction on all trajectories within the dynamic system, irrespective of the initial conditions. This implies that, irrespective of the specific set of initial conditions, the system's state will inevitably converge towards the equilibrium point $E^*$ over time.

## 5 Transcritical bifurcation

According to Theorem 1, the equilibrium $E_3$ is locally asymptotically stable when $\pi_2 > (\pi_1 k B_3 - \pi_0)/I_3$ and unstable when $\pi_2 < (\pi_1 k B_3 - \pi_0)/I_3$. Furthermore, for $\pi_2 < (\pi_1 k B_3 - \pi_0)/I_3$, we get an unique interior equilibrium of system (1). Thus, $\pi_2 = \pi_2^* = (\pi_1 k B_3 - \pi_0)/I_3$ is a critical point, where transcritical bifurcation can occur around the boundary equilibrium $E_3$. Using technique discussed in [3], we assert the following theorem containing the result associated with the manifestation of transcritical bifurcation.

**Theorem 3.** *System* (1) *displays transcritical bifurcation at $\pi_2 = \pi_2^*$ around the equilibrium $E_3$ in the backward direction.*

*Proof.* The Jacobian matrix $J_{E_3}$ possesses a zero eigenvalue at $\pi_2 = \pi_2^* = (\pi k B_3 - \pi_0)/I_3$, which implies that $E_3$ is nonhyperbolic. To analyze the behavior of system (1) at $\pi_2 = \pi_2^*$, we employ the theory discussed in [3]. To proceed, we evaluate the values of $a$ and $b$ as described in [3]. Let $F = y_1$, $B = y_2$, $I = y_3$, and $W = y_4$ and take $\pi_2$ as bifurcation parameter. Thus, we can rewrite the right-hand side of the formulated system (1) in the following form:

$$\begin{aligned}
\tilde{g}_1 &= q - \alpha_0(y_1 - F_0) - \alpha_1 y_3 y_1, \\
\tilde{g}_2 &= s y_1 - s_0 y_2 - k y_2 y_4, \\
\tilde{g}_3 &= \mu\alpha_1 y_3 y_1 - \mu_0 y_3^2, \\
\tilde{g}_4 &= \pi k y_2 y_4 - \pi_0 y_4 - \pi_1 y_4^2 - \pi_2 y_4 y_3.
\end{aligned}$$

Let $U$ and $V$ denote the right and left eigenvectors corresponding to zero eigenvalue of the Jacobian matrix $J_{(E_3,\pi_2^*)}$. We have obtained these eigenvectors as follows:

$$U = \begin{bmatrix} -\alpha_1 k F_3 B_3 \\ k B_3 \\ (\alpha_0 + \alpha_1 F_3) k B_3 \\ -s_0 - s\alpha_1 F_3 \end{bmatrix} \quad \text{and} \quad V = \begin{bmatrix} \mu\alpha_1 F_3 - 2\mu_0 I_3 \\ 0 \\ \alpha_1 F_3 \\ 1 \end{bmatrix}^{\mathrm{T}}.$$

For system (1), $a$ and $b$ are as follows:

$$a = \sum_{n,i,j=1}^{4} v_n u_i u_j \frac{\partial^2 \tilde{g}_n}{\partial y_i \partial y_j}(E_3, \pi_2^*) \quad \text{and} \quad b = \sum_{n,i=1}^{4} v_n u_i \frac{\partial^2 \tilde{g}_n}{\partial y_i \partial \pi_2}(E_3, \pi_2^*),$$

where $u_i$s' and $v_i$s' ($i = 1, 2, 3, 4$) are the components of eigenvectors $U$ and $V$, respectively. We have obtained the values of $a$ and $b$ for system (1) as follows:

$$\begin{aligned} a &= 2\alpha_1^2 k^2 F_3 B_3^2 (\mu\alpha_1 F_3 - 2\mu_0 I_3)(\alpha_0 + \alpha_1 I_3) - 2\alpha_1^2 k^2 F_3 B_3^2 (\alpha_0 + \alpha_1 I_3) \\ &\quad - 2\mu_0 \alpha_1 F_3 \big((\alpha_0 + \alpha_1 I_3) k B_3\big)^2 + 2\pi k^2 B_3 (s\alpha_1 F_3 + s_0) \\ &\quad + 2\pi_2 k B_3 (\alpha_0 + \alpha_1 I_3)(s_0 + s\alpha_1 F_3) - 2\pi (s\alpha_1 F_3 + s_0)^2 \end{aligned}$$

and

$$b = \delta(s_0 + s\alpha_1 F_3) I_3 > 0,$$

According to statements (i) and (iv) of Theorem 1, as discussed in [3], we can conclude that the system described by (1) exhibits transcritical bifurcation at $\pi_2 = \pi_2^*$ around $E_3$ in the forward direction when $a < 0$ and in the backward direction when $a > 0$. After some algebraic simplifications, we get that $a > 0$, therefore, system (1) exhibits transcritical bifurcation in backward direction. □

## 6 Numerical simulation

Now, we conduct numerical simulations for model (1) to validate feasibility of the analytical results, employing a specified set of parameter values as follows: $F_0 = 100$, $q = 10$, $\alpha_0 = 0.05$, $\alpha_1 = 0.004$, $s = 2$, $s_0 = 0.07$, $\mu = 0.4$, $\mu_0 = 0.01$, $\pi = 0.6$, $\pi_0 = 0.02$, $\pi_1 = 0.01$, $\pi_2 = 0.01$, $k = 0.01$. The components of equilibrium $E^*$ are derived as

$$F^* = 118.93, \qquad B^* = 211.14, \qquad I^* = 19.02, \qquad W^* = 105.65.$$

Additionally, the eigenvalues of the Jacobian matrix associated with the equilibrium $E^*$ mentioned above are calculated as

$$\begin{aligned} &-0.1582 + 0.1159\mathrm{i}, \quad -0.1582 - 0.1159\mathrm{i}, \\ &-1.0915 + 1.1564\mathrm{i}, \quad -1.0915 - 1.1564\mathrm{i}. \end{aligned}$$

All eigenvalues exhibit either negativity or a negative real part, signifying the local asymptotic stability of $E^*$ under the provided parameter values. Figure 2 visually confirms this observation, revealing that trajectories originating from any point consistently converge towards the equilibrium state $E^*$. This evidence establishes the global asymptotic stability of $E^*$. Figure 3 illustrates a transcritical bifurcation in the system, showing how the migration rate coefficient $\pi_2$ influences the stability of wildlife populations, depending on the growth rate of wildlife $\pi$. The plot demonstrates how small changes in industrialization ($\pi_2$) can cause significant shifts in system dynamics, affecting wildlife population stability. It highlights the delicate balance between ecological stability and human-induced pressures, such as migration and habitat loss, and emphasizes the need for careful management to avoid destabilizing wildlife populations. The impact of $k$ on the stability of equilibrium $E_3$ is illustrated in Fig. 4. According to Theorem 1, equilibrium $E_3$ remains stable when $\pi_2$ is less than $\pi_2^* = (\pi k B_3 - \pi_0)/I_3$; otherwise, it transitions

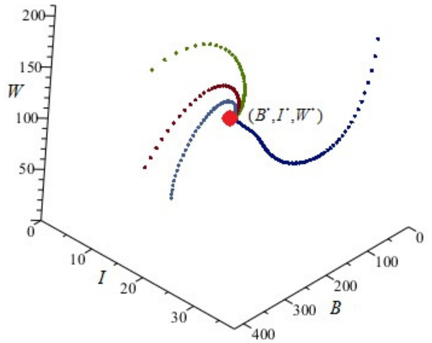


**Figure 2.** Global stability of the interior equilibrium $E^*$ in $BIW$-space.

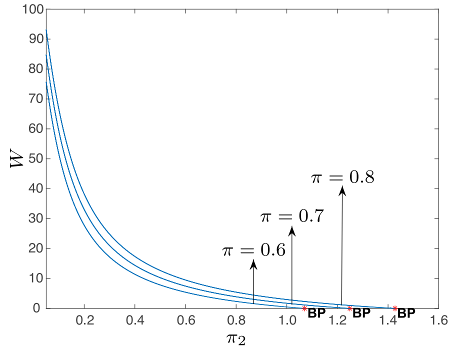


**Figure 3.** Plot of transcritical bifurcation with respect to $\pi_2$ for different values of $\pi$.

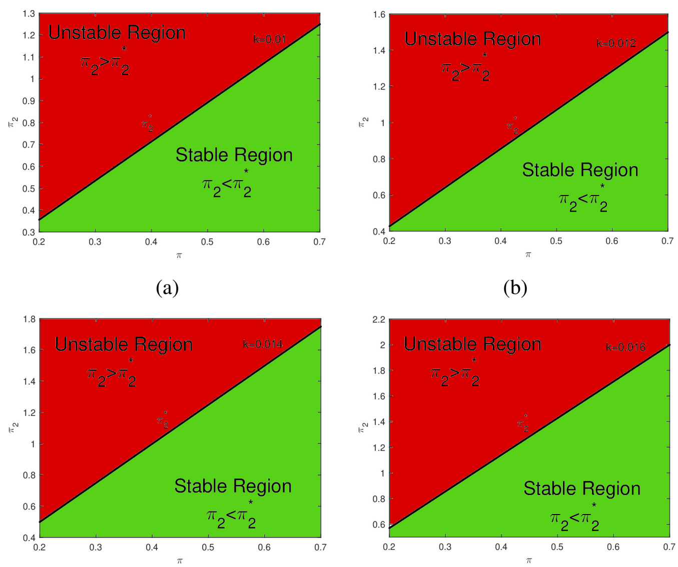


(a) (b) (c) (d)

**Figure 4.** Effect of $k$ on the stability region of $E_3$ with all other parameter values are same.

to an unstable state. In this figure, the red region highlights the parametric space where $\pi_2 > \pi_2^*$, indicating instability in $E_3$. Conversely, the green region signifies the parametric space where $\pi_2 < \pi_2^*$, ensuring the stability of $E_3$. Notably, the figure reveals that as the predation rate of the animal species increases, the stability region of equilibrium $E_3$ expands, underscoring the sensitivity of the system to changes in predation dynamics.

Figures 5–10 depict how variables change over time for different values of important parameters. Specifically, at various rates of forest area depletion caused by industrializa-

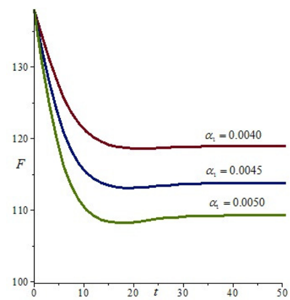


**Figure 5.** Variation of $F$ with $\alpha_1$.

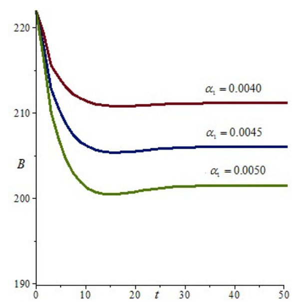


**Figure 6.** Variation of $B$ with $\alpha_1$.

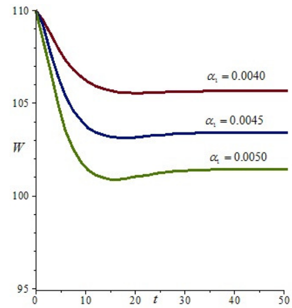


**Figure 7.** Variation of $W$ with $\alpha_1$.

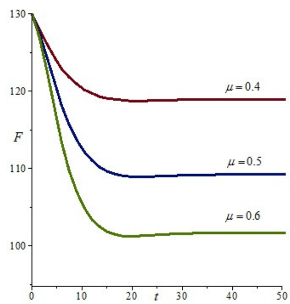


**Figure 8.** Variation of $F$ with $\mu$.

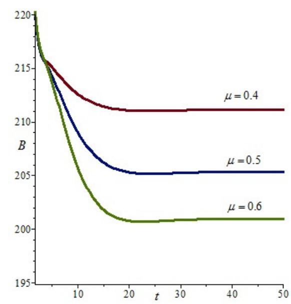


**Figure 9.** Variation of $B$ with $\mu$.

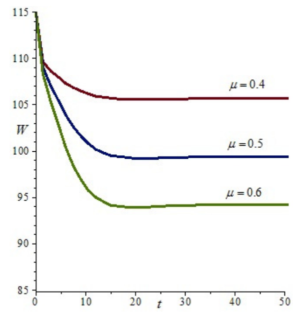


**Figure 10.** Variation of $W$ with $\mu$.

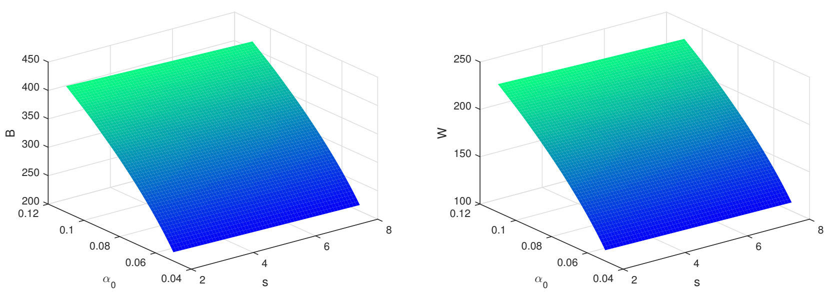


(a) (b)

**Figure 11.** Surface plots of the biomass density, wildlife species with respect to $s$, $\alpha_0$.

tion, Figs. 5–7 illustrate the changes in forest area, cumulative density of forest resources, and population density of animal species over time $t$. The data unambiguously demonstrate a clear trend: there is a simultaneous decline in forest area, cumulative density of forest resources, and population density of animal species as the pace of forest area depletion due to industrialization increases. For various values of the proportionality constant $\mu$ (which indicates the growth rate of industrialization driven by forest area), Figs. 8–10 display the dynamics of forest area, cumulative density of forest resources, and population density of wildlife species over period $t$. These graphs unequivocally show that a rise in the rate proportionality constant $\mu$ corresponds to a simultaneous decline in the cumulative density of forest resources, the population density of animal species, and the area covered by forests. Therefore, it is evident from the preceding discussion that industrialization's growth is a major cause of the deterioration of forest regions, as well as the loss of forest resources and the emigration of wildlife that depends on them. Figures 5–10 offer policymakers valuable insights into the impacts of industrialization on forest area, biomass, and wildlife. If increasing industrial impact ($\alpha_1$) leads to reductions in forest area and biomass and a decline in wildlife density, policy should focus on regulating industrial activities to protect forests and maintain biomass resources. Similarly, if industrialization level ($\mu$) negatively affects forest area, biomass, and wildlife, measures such as stricter zoning, sustainable industrial practices, and the creation of wildlife corridors and protected areas are essential to mitigate environmental degradation. These results underscore the importance of balancing industrial growth with conservation strategies to preserve ecosystems and biodiversity.

In Fig. 11, we explore the simultaneous variation of two key parameters in model (1) to understand their influence on both biomass density and wildlife populations in the region. The surface plots provide a clear visualization of the equilibrium levels for these variables as the selected parameters. For biomass density, its equilibrium is shaped by the growth rate and the depletion rate due to natural factors, illustrating how these elements collectively drive biomass stability. Meanwhile, the equilibrium level of wildlife species, which grows at a rate $\alpha_0$, is also sensitive to the biomass growth rate, denoted by $s$, as it serves as a vital resource for wildlife. These plots offer a powerful view of the interdependencies between biomass and wildlife, highlighting the delicate balance sustained within the ecosystem.

## 7 Sensitivity analysis

A semirelative sensitivity analysis was performed on model system (1) to assess how changes in parameter values affect model variables. This approach highlights the responsiveness of each variable, identifying key parameters that most influence system dynamics [2]. Let $X_w$ represent the sensitivity function of the state variable $X$ with respect to $w$, defined as $X_w(t) = \partial X(t,w)/\partial w$. For the sensitivity analysis, the parameters $\alpha_1$, $k$, $\mu_0$, and $\pi$ are selected as the key sensitive parameters. The corresponding sensitivity equations for these parameters are given as follows:

$$\begin{aligned}\dot{F}_{\alpha_1}(t,\alpha_1) &= -\alpha_0 F_{\alpha_1}(t,\alpha_1) - F(t,\alpha_1)I(t,\alpha_1)\\ &\quad - \alpha_1 F(t,\alpha_1)I_{\alpha_1}(t,\alpha_1) - \alpha_1 F_{\alpha_1}(t,\alpha_1)I(t,\alpha_1),\\ \dot{B}_{\alpha_1}(t,\alpha_1) &= sF_{\alpha_1}(t,\alpha_1) - s_0 B_{\alpha_1}(t,\alpha_1)\\ &\quad - kB_{\alpha_1}(t,\alpha_1)W(t,\alpha_1) - kB(t,\alpha_1)W_{\alpha_1}(t,\alpha_1),\end{aligned}$$

$$\begin{aligned}
\dot{I}_{\alpha_1}(t,\alpha_1) &= \mu F(t,\alpha_1)I(t,\alpha_1) + \mu\alpha_1 F(t,\alpha_1)I_{\alpha_1}(t,\alpha_1) \\
&\quad + \mu\alpha_1 F_{\alpha_1}(t,\alpha_1)I(t,\alpha_1) - 2\mu_0 I(t,\alpha_1)I_{\alpha_1}(t,\alpha_1), \\
\dot{W}_{\alpha_1}(t,\alpha_1) &= \pi k B(t,\alpha_1)W_{\alpha_1}(t,\alpha_1) + \pi k B_{\alpha_1}(t,\alpha)W(t,\alpha_1) \\
&\quad - \pi_0 W_{\alpha_1}(t,\alpha_1) - 2\pi_1 W(t,\alpha_1)W_{\alpha_1}(t,\alpha_1) \\
&\quad - \pi_2 I_{\alpha_1}(t,\alpha_1)W(t,\alpha_1) - \pi_2 I(t,\alpha_1)W_{\alpha_1}(t,\alpha_1);
\end{aligned}$$

$$\begin{aligned}
\dot{F}_k(t,k) &= -\alpha_0 F_k(t,k) - \alpha_1 F(t,k)I_k(t,k) - \alpha_1 F_k(t,k)I(t,k), \\
\dot{B}_k(t,k) &= sF_k(t,k) - s_0 B_k(t,k) - F(t,k)I(t,k) \\
&\quad - kB_k(t,k)W(t,k) - kB(t,k)W_k(t,k), \\
\dot{I}_k(t,k) &= \mu\alpha_1 F(t,k)I_k(t,k) + \mu\alpha_1 F_k(t,k)I(t,k) - 2\mu_0 I(t,k)I_k(t,k), \\
\dot{W}_k(t,k) &= \pi B(t,k)W(t,k) + \pi k B(t,k)W_k(t,k) + \pi k B_k(t,k)W(t,k) \\
&\quad - \pi_0 W_k(t,k) - 2\pi_1 W(t,k)W_k(t,k) \\
&\quad - \pi_2 I_k(t,k)W(t,k) - \pi_2 I(t,k)W_k(t,k);
\end{aligned}$$

$$\begin{aligned}
\dot{F}_{\mu_0}(t,\mu_0) &= -\alpha_0 F_{\mu_0}(t,\mu_0) - \alpha_1 F(t,\mu_0)I_{\mu_0}(t,\mu_0) - \alpha_1 F_{\mu_0}(t,\mu_0)I(t,\mu_0), \\
\dot{B}_{\mu_0}(t,\mu_0) &= sF_{\mu_0}(t,\mu_0) - s_0 B_{\mu_0}(t,\mu_0) \\
&\quad - kB_{\mu_0}(t,\mu_0)W(t,\mu_0) - kB(t,\mu_0)W_{\mu_0}(t,\mu_0), \\
\dot{I}_{\mu_0}(t,\mu_0) &= \mu\alpha_1 F(t,\mu_0)I_{\mu_0}(t,\mu_0) + \mu\alpha_1 F_{\mu_0}(t,\mu_0)I(t,\mu_0) \\
&\quad - I(t,\mu_0)I(t,\mu_0) - 2\mu_0 I(t,\mu_0)I_{\mu_0}(t,\mu_0), \\
\dot{W}_{\mu_0}(t,\mu_0) &= \pi k B(t,\mu_0)W_{\mu_0}(t,\mu_0) + \pi k B_{\mu_0}(t,\mu_0)W(t,\mu_0) \\
&\quad - \pi_0 W_{\mu_0}(t,\mu_0) - 2\pi_1 W(t,\mu_0)W_{\mu_0}(t,\mu_0) \\
&\quad - \pi_2 I_{\mu_0}(t,\mu_0)W(t,\mu_0) - \pi_2 I(t,\mu_0)W_{\mu_0}(t,\mu_0);
\end{aligned}$$

$$\begin{aligned}
\dot{F}_\pi(t,\pi) &= -\alpha_0 F_\pi(t,\pi) - \alpha_1 F(t,\pi)I_\pi(t,\pi) - \alpha_1 F_\pi(t,\pi)I(t,\pi), \\
\dot{B}_\pi(t,\pi) &= sF_\pi(t,\pi) - s_0 B_\pi(t,\pi) - kB_\pi(t,\pi)W(t,\pi) - kB(t,\pi)W_\pi(t,\pi), \\
\dot{I}_\pi(t,\pi) &= \mu\alpha_1 F(t,\pi)I_\pi(t,\pi) + \mu\alpha_1 F_\pi(t,\pi)I(t,\pi) - 2\mu_0 I(t,\pi)I_\pi(t,\pi), \\
\dot{W}_\pi(t,\pi) &= kB(t,\pi)W(t,\pi) + \pi k B(t,\pi)W_\pi(t,\pi) + \pi k B_\pi(t,\pi)W(t,\pi) \\
&\quad - \pi_0 W_\pi(t,\pi) - 2\pi_1 W(t,\pi)W_\pi(t,\pi) \\
&\quad - \pi_2 I_\pi(t,\pi)W(t,\pi) - \pi_2 I(t,\pi)W_\pi(t,\pi).
\end{aligned}$$

Figure 12 presents the semirelative sensitivity solutions, illustrating the impact of doubling key parameters $\alpha_1$, $k$, $\mu_0$, and $\pi$ on various model variables in system (1). Among these parameters, the intraspecific competition coefficient among industries, $\mu_0$, drives the most significant increase in both forest area and biomass density, underscoring its influence on resource availability and environmental sustainability. Parameters $\alpha_1$ and $\pi$ similarly prompt the greatest increases in industrialization and wildlife species, indicating their strong association with growth dynamics in these sectors. Conversely, we

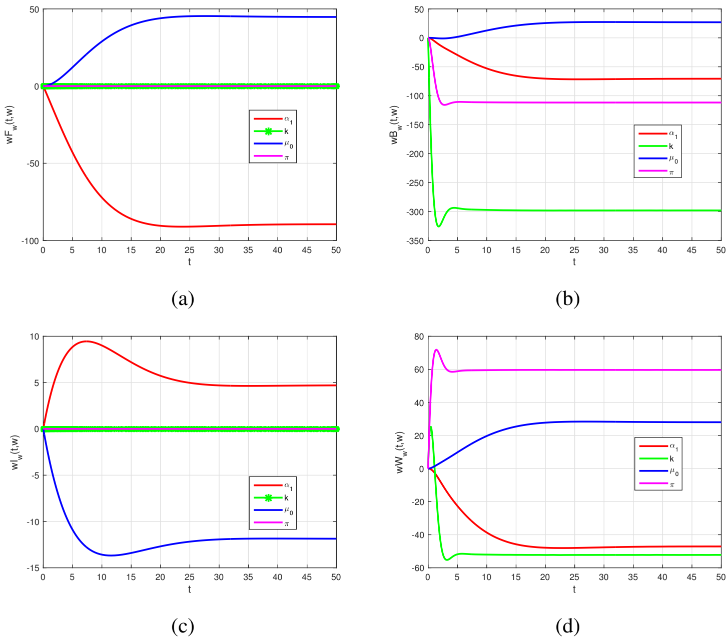


**Figure 12.** Sensitivity solutions of semirelative type for dynamic variables $F$, $B$, $I$, and $W$ with respect to parameters $\alpha_1$, $k$, $\mu_0$, and $\pi$.

observe that parameters $\alpha_1$, $\mu_0$, and $k$ lead to the most substantial declines in forest area, industrialization, biomass density, and wildlife species, reflecting their complex roles in resource depletion and ecosystem.

# 8 Conclusion

The degradation of forests from industrialization forces wildlife to migrate, disrupting ecosystems and threatening biodiversity. Habitat loss compels species to seek new environments, often leading to human–wildlife conflicts. This destabilizes ecosystems and undermines essential ecological services. Sustainable practices and conservation efforts are crucial to mitigate these impacts and preserve forest habitats.

This study examines the effects of forest degradation from industrialization on wildlife migration. The model integrates four variables: wildlife population density $W(t)$, industrialization level $I(t)$, cumulative biomass density $B(t)$, and forest area $F(t)$. It is assumed that forest biomass density is proportional to forest area and that industrialization depletes resources, intensifying intraspecific competition and driving wildlife migration. A qualitative analysis using stability theory for differential equations is conducted, supported by numerical simulations, sensitivity analysis, and graphical representations to explore variable dynamics under different parameter settings. Further, the study reveals that wildlife migration is highly sensitive to industrialization and biomass loss. As industrial activity increases, forest area and biomass decline, accelerating migration. This disruption heightens species competition and may cause instability or local extinction. The model identifies thresholds where ecological balance shifts, stressing the need for sustainable industry and conservation. It urges policymakers to protect habitats and curb industrial encroachment to preserve biodiversity and ecosystem stability. It is noted that possible extensions of the model include incorporating climate change effects, human population dynamics, and ecosystem services to examine how environmental changes and urbanization influence forest and wildlife.

**Author contributions.** All authors (S.J., S.S., and A.M.) have contributed as follows: methodology, S.J.; model formulation and analysis, S.J. and S.S.; numerical simulations, A.M.; writing – original draft praparation, S.J., S.S., and A.M. All authors have reviewed and approved the final manuscript.

**Conflicts of interest.** The authors declare no conflicts of interest.

## References

1. M. Agarwal, T. Fatima, H.I. Freedman, Depletion of forestry resource biomass due to industrialization pressure: A ratio-dependent mathematical model, *J. Biol. Dyn.*, **4**(4):381–396, 2010, https://doi.org/10.1080/17513750903326639.
2. D.M. Bortz, P.W. Nelson, Sensitivity analysis of a nonlinear lumped parameter model of HIV infection dynamics, *Bull. Math. Biol.*, **66**(5):1009–1026, 2004, ISSN 0092-8240, https://doi.org/10.1016/j.bulm.2003.10.011.
3. C. Castillo-Chavez, B. Song, Dynamical models of tuberculosis and their applications, *Math. Biosci. Eng.*, **1**(2):361–404, 2004, https://doi.org/10.3934/mbe.2004.1.361.
4. B. Dubey, S. Sharma, P. Sinha, J.B. Shukla, Modelling the depletion of forestry resources by population and population pressure augmented industrialization, *Appl. Math. Modelling*, **33**(7): 3002–3014, 2009, https://doi.org/10.1016/j.apm.2008.10.028.
5. B. Dubey, R.K. Upadhyay, J. Hussain, Effects of industrialization and pollution on resource biomass: A mathematical model, *Ecol. Modelling*, **167**(1):83–95, 2003, https://doi.org/10.1016/S0304-3800(03)00168-6.
6. I.M. Fanuel, D. Kajunguri, F. Moyo, Modelling the impact of human population and its associated pressure on forest biomass and forest-dependent wildlife population, *J. Appl. Math.*, **2023**(1):4826313, 2023, https://doi.org/10.1155/2023/4826313.
7. H.I. Freedman, J.H. So, Global stability and persistence of simple food chains, *Math. Biosci.*, **76**(1):69–86, 1985, https://doi.org/10.1016/0025-5564(85)90047-1.
8. A. Jha, A.K. Misra, A robust role of carbon taxes towards alleviating carbon dioxide: A modeling study, *J. Eng. Math.*, **144**(1):20, 2024, https://doi.org/10.1007/s10665-023-10327-x.
9. K. Jyotsna, A. Tandon, A mathematical model studying the survival of forest resource dependent wildlife population in the presence of population pressure induced mining activities, *Nat. Resour Model.*, **30**(4):e12139, 2017, https://doi.org/10.1111/nrm.12139.

10. K. Lata, B. Dubey, A.K. Misra, Modeling the effects of wood and non-wood based industries on forestry resources, *Nat. Resour. Model.*, **29**(4):559–580, 2016, https://doi.org/10.1111/nrm.12111.

11. K. Lata, A.K. Misra, J.B. Shukla, Modeling the effect of deforestation caused by human population pressure on wildlife species, *Nonlinear Anal., Real World Appl.*, **23**(3):303–320, 2018, https://doi.org/10.15388/NA.2018.3.2.

12. S. Mangla, S. Sharma, R. Boadh, Y.K. Rajoria, A mathematical model of the impact of deforestation on the growth of forest resources, *Neuroquantology*, **20**(17):223, 2022, https://doi.org/10.14704/Nq.2022.20.17.Nq88030.

13. A. K. Misra, K. Lata, J.B. Shukla, A mathematical model for the depletion of forestry resources due to population and population pressure augmented industrialization, *Int. J. Model. Simul. Sci. Comput.*, **05**(01):1350022, 2014, https://doi.org/10.1142/S1793962313500220.

14. A.K. Misra, A. Jha, Modeling the effect of population pressure on the dynamics of carbon dioxide gas, *J. Appl. Math. Comput*, **67**(1):623–640, 2021, https://doi.org/10.1007/s12190-020-01492-8.

15. A.K. Misra, A. Jha, How to combat atmospheric carbon dioxide along with development activities? A mathematical model, *Physica D*, **454**:133861, 2023, https://doi.org/10.1016/j.physd.2023.133861.

16. R. Pathak, Depletion of forest resources and wildlife population with habitat complexity: A mathematical model, *Open J. Ecol.*, **8**(11):579, 2018, https://doi.org/10.4236/oje.2018.811034.

17. V. Ramdhani, E. H. Nugrahani, Dynamical system of modelling the depletion of forestry resources due to crowding by industrialization, *Appl. Math. Sci.*, **9**(82):4067–4079, 2015, https://doi.org/10.12988/ams.2015.53259.

18. J. B. Shukla, K. Lata, A. K. Misra, Modeling the depletion of a renewable resource by population and industrialization: Effect of technology on its conservation, *Nat. Resour. Model.*, **24**(2):242–267, 2011, https://doi.org/10.15388/NA.2017.4.4.

19. J.B. Shukla, B. Dubey, H.I. Freedman, Effect of changing habitat on survival of species, *Ecol. Modell.*, **87**(1):205–216, 1996, https://doi.org/10.1016/0304-3800(95)00029-1.

20. S. K. Sinha, J. Pal, K. Jyotsna, A dynamical study on the adverse effects of industrial activities in the forest and wildlife region through modelling, *Model. Earth Syst. Environ.*, **9**(2):2053–2065, 2023, https://doi.org/10.1007/s40808-022-01581-6.

21. I. Skrynetska, R. Ciepał, M. Kandziora-Ciupa, G. Barczyk, A. Nadgórska-Socha, Ecophysiological responses to environmental pollution of selected plant species in an industrial urban area, *Int. J. Environ. Res.*, **12**:255–267, 2018, https://doi.org/10.1007/s41742-018-0088-9.

22. J. Talberth, D. DellaSala, E. Fernandez, Global forest watch report, *Wilderness*, **503**:657–7336, 2015.

23. A. Verma, M.S. Arora, A. Omar, K. Chauhan, Optimal control of global warming by carbon dioxide mitigation through awareness programmes, *Int. J. Environ. Res.*, **18**:55, 2024, https://doi.org/10.1007/s41742-024-00606-5.

24. M.A. Zahed, M. Hadipour, G. Mastali, M. Esmaeilzadeh, A. Mojiri, Simultaneous ecosystem benefit and climate change control: A future study on sustainable development in Iran, *Int. J. Environ. Res.*, **16**:28, 2022, https://doi.org/10.1007/s41742-022-00410-z.

25. Deforestation and Forest Degradation, World Wildlife Fund (WWF), https://www.worldwildlife.org/threats/deforestation.

26. IPCC, 2019: Summary for Policymakers, in P.R. Shukla et al. (Ed.), *Climate Change and Land: IPCC Special Report on Climate Change, Desertification, Land Degradation, Sustainable Land Management, Food Security, and Greenhouse Gas Fluxes in Terrestrial Ecosystems*, Cambridge Univ. Press, Cambridge, 2022, pp. 1–36, https://doi.org/10.1017/9781009157988.001.

27. The State of the World's Forests 2020: Forests, Biodiversity and People, Food and Agriculture Organization of the United Nations (FAO), 2020, https://www.fao.org/state-of-forests/en/.

28. The World Bank in Forestry, World Bank, 2020, https://www.worldbank.org/en/topic/forestry/overview.